

# 1 Title: Waves of chromatin modifications in mouse dendritic 2 cells in response to LPS stimulation

3 **Authors:** Alexis Vandenberg<sup>1§\*</sup>, Yutaro Kumagai<sup>2§</sup>, Mengjie Lin<sup>3</sup>, Yutaka Suzuki<sup>3</sup>, Kenta Nakai<sup>4\*</sup>

4 <sup>1</sup> Immuno-Genomics Research Unit, Immunology Frontier Research Center (IFReC), Osaka University,  
5 Suita, 565-0871, Japan

6 <sup>2</sup> Quantitative Immunology Research Unit, Immunology Frontier Research Center (IFReC), Osaka  
7 University, Suita, 565-0871, Japan

8 <sup>3</sup> Department of Computational Biology and Medical Sciences, Graduate School of  
9 Frontier Sciences, The University of Tokyo, Kashiwa 277-8561, Japan

10 <sup>4</sup> Laboratory of Functional Analysis in silico, The Institute of Medical Science, The University of Tokyo,  
11 Minato-ku, Tokyo, 108-8639, Japan

12 § Equal contribution

13 \* To whom correspondence should be addressed. Email: [alexisvdb@ifrec.osaka-u.ac.jp](mailto:alexisvdb@ifrec.osaka-u.ac.jp),  
14 [knakai@ims.u-tokyo.ac.jp](mailto:knakai@ims.u-tokyo.ac.jp)

15

## 16 Abstract

17 **Background:** The importance of transcription factors (TFs) and epigenetic modifications in the  
18 control of gene expression is widely accepted. However, causal relationships between changes in TF  
19 binding, histone modifications, and gene expression during the response to extracellular stimuli are  
20 not well understood. Here, we analyzed the ordering of these events on a genome-wide scale in  
21 dendritic cells (DCs) in response to lipopolysaccharide (LPS) stimulation.

22 **Results:** Using a ChIP-seq time series dataset, we found that the timing of H3K27ac accumulation at  
23 promoters coincided with their transcriptional induction. However, in contrast, the LPS-induced

24 accumulation of several other histone modifications at promoters and enhancers occurred in “waves”  
25 within specific time frames after stimulation, independent of the timing of transcriptional induction.  
26 Integrative analysis with TF binding data revealed potential links between the timing of TF activation  
27 and accumulation of histone modifications. Especially, binding by STAT1/2 coincided with induction  
28 of H3K9K14ac, and was followed by increases in H3K4me3. In a subset of LPS-induced genes the  
29 induction of these modifications was found to be TRIF-, IRF3-, and IFNR-dependent, further  
30 supporting a role for STAT1/2 in the regulation of these histone modifications.

31 **Conclusions:** The timing of several stimulus-induced, short-term changes in histone modifications  
32 appears to be relatively independent of dynamics in activity of regulatory regions. This suggests a  
33 lack of a direct causal relationship. Changes in these modifications more likely reflect the activation  
34 of stimulus-dependent TFs and their interactions with chromatin modifiers.

35 **Running title:** Waves of chromatin modification in immune response

36 **Keywords:** histone modifications, dendritic cells, epigenetics, transcription factors, ChIP-seq, time  
37 series

## 38 Background

39 Epigenetic features, such as covalent post-translational modifications of histone proteins and DNA  
40 methylation, are thought to play a crucial role in controlling the accessibility of DNA to RNA  
41 polymerases. Associations have been found between histone modifications and both long-term and  
42 short-term cellular processes, including development, heritability of cell type identity, DNA repair,  
43 and transcriptional control [1,2]. For cells of the hematopoietic lineage, cell type-defining enhancers  
44 are thought to be established during the process of differentiation from stem cells by priming with  
45 the H3K4me1 marker [3,4]. On the other hand, in differentiated cells, extracellular stimuli are  
46 accompanied by relatively short-term or transient changes in histone modifications reflecting the  
47 changes in activity of enhancers and promoters [5–7].

48 TFs are key regulators in the control of epigenetic changes [8,9]. During the long-term process of  
49 development, closed chromatin is first bound by pioneer TFs, which results in structural changes that  
50 make it accessible to other TFs and RNA polymerase II (Pol2) [7,10]. Similarly, more short-term  
51 changes in gene expression following stimulation of immune cells are regulated by TFs. This  
52 regulation is thought to involve TF binding, induction of changes in histone modifications, and  
53 recruitment of Pol2 [11–14]. However, details of the temporal ordering and causal relationships  
54 between these events remain poorly understood [15,16]. Especially, it is unclear whether certain  
55 histone modifications are a requirement for, or a result of, TF binding and transcription [17–19].

56 As sentinel cells of the innate immune system, DCs are well equipped for detecting the presence of  
57 pathogens. Lipopolysaccharide (LPS), a component of the cell wall of Gram negative bacteria, is  
58 recognized by DCs through the membrane-bound Toll-like receptor 4 (TLR4), resulting in the  
59 activation of two downstream signaling pathways [20]. One pathway is dependent on the adaptor  
60 protein MyD88, and leads to the activation of the TF NF- $\kappa$ B, which induces expression of  
61 proinflammatory cytokines. The other pathway involves the receptor protein TRIF, whose activation  
62 induces phosphorylation of the TF IRF3 by TBK1 kinase. The activated IRF3 induces expression of

63 type I interferon, which in turn activates the JAK-STAT signaling pathway, by binding to the type I IFN  
64 receptor (IFNR) [21].

65 Here, we present a large-scale study of short-term changes in histone modifications in mouse DCs  
66 during the response to LPS. We focused on the timing of accumulation of histone modifications at  
67 promoters and enhancers, relative to the induction of transcription and to TF binding events. We  
68 observed that LPS stimulation induced increased levels of H3K9K14ac, H3K27ac, H3K4me3 and  
69 H3K36me3 at LPS-induced promoters and enhancers. However, surprisingly, we found that the  
70 accumulation of H3K9K14ac (between 0.5 and 3 hours) and H3K4me3 (between 2 and 4 hours)  
71 occurred within specific time frames after stimulation, independent of the timing of transcriptional  
72 induction of nearby genes. This finding suggests a lack of a direct causal relation between increases  
73 in these markers and induction of gene expression. H3K36me3 in LPS-induced genes spreads from  
74 the 3' end of gene bodies towards the 5' end, reaching promoters at later time points (between 8  
75 and 24 hours). Integrated analysis of induction times of histone modifications with genome-wide  
76 binding data for 24 TFs revealed possible associations between increases in H3K9K14ac and  
77 H3K4me3 and binding by Rel $\alpha$ , Irf1, and especially STAT1/2. For STAT1/2, this association was further  
78 supported using independent ChIP-qPCR experiments in TRIF<sup>-/-</sup>, IRF3<sup>-/-</sup>, and IFNR<sup>-/-</sup> cells, and in wild  
79 type (WT) and TRIF<sup>-/-</sup> cells stimulated with IFN- $\beta$ . Together, these results suggest that accumulation  
80 of histone modification within specific time windows reflects the timing of activation of stimulus-  
81 dependent TFs, and that the accumulation of H3K9K14ac and H3K4me3 is neither an absolute  
82 requirement for, nor a direct result of, stimulus-dependent transcriptional induction.

## 83 Results

### 84 Genome-wide Measurement of Histone Modifications at Promoter and Enhancer

#### 85 Regions

86 To elucidate the temporal ordering of stimulus-induced changes in transcription and chromatin  
87 structure, we performed chromatin immunoprecipitation experiments followed by high-throughput  
88 sequencing (ChIP-seq) for the following histone modifications in mouse DCs before and after LPS  
89 stimulation: H3K4me1, H3K4me3, H3K9K14ac, H3K9me3, H3K27ac, H3K27me3, H3K36me3, and  
90 similarly for Pol2 (Fig. S1), for ten time points (0h, 0.5h, 1h, 2h, 3h, 4h, 6h, 8h, 16h, 24h). We  
91 integrated this data with publicly available whole-genome transcription start site (TSS) data (TSS-  
92 seq) [22]. All data originated from the same cell type, treated with the same stimulus, and samples  
93 taken at the same time points.

94 Using this data collection, we defined 24,416 promoters (based on TSS-seq data and Refseq  
95 annotations) and 34,079 enhancers (using H3K4me1<sup>high</sup>/H3K4me3<sup>low</sup> signals) (see Methods). For this  
96 genome-wide set of promoters and enhancers, we estimated the levels of histone modifications,  
97 Pol2 binding, and RNA reads over time (see Methods).

#### 98 Epigenetic Changes at Inducible Promoters and their Enhancers

99 Recent studies using the same cell type and stimulus showed that most changes in gene expression  
100 patterns were controlled at the transcriptional level, without widespread changes in RNA  
101 degradation rates [23,24]. We therefore defined 1,413 LPS-induced promoters based on increases in  
102 TSS-seq reads after LPS stimulation, and inferred their transcriptional induction time (see Methods).  
103 Fig. 1A shows changes in transcriptional activity of LPS-induced promoters. In addition to a relatively  
104 large number of immediate-early induced promoters (0.5h, 259 promoters) and promoters with very  
105 late induction (24h, 299 promoters), at each time point we observed between 85 to 180 induced

106 promoters. In addition, we defined a set of 772 promoters with highly stable activity over the entire  
107 time course (see Methods).

108 A previous study suggested only limited dynamics of histone modifications at stimulus-induced  
109 promoters in mouse DCs, based on data taken at a few time points [25]. Our dataset, however,  
110 allows the analysis of the timing of changes over an extended time period after stimulation.

111 For both promoters and enhancers, we defined significant increases in histone modifications and  
112 Pol2 binding by comparison to pre-stimulation levels (see Methods). Our analysis suggested that  
113 changes were in general rare; only 0.7 to 5.3 % of all promoters (Fig. 1B) and 0.2 to 11.0 % of all  
114 enhancers (Fig. 1C) experienced significant increases in histone modifications and Pol2 binding.

115 Changes at the promoters and enhancers of stably active promoters were similarly rare (not shown).

116 However, changes were found relatively frequently at LPS-induced promoters, especially for markers  
117 of activity such as Pol2 binding, H3K4me3, H3K27ac, and H3K9K14ac, as well as for H3K36me3 (Fig.

118 1B). For example, while only 957 promoters (out of a total of 24,416 promoters; 3.9%) experienced

119 significant increases in H3K9K14ac, this included 27.6% of the LPS-induced promoters (390 out of

120 1,413 promoters). To a lesser extent, we observed the same tendency at associated enhancers (Fig.

121 1C). The smaller differences at enhancers are likely to be caused by imperfect assignments of

122 enhancers to LPS-induced promoters (i.e. we naively assigned enhancers to their most proximal  
123 promoter).

124 LPS-induced promoters were less frequently associated with CpG islands (57%) than stably

125 expressed promoters (87%, Fig. S2A) [26]. Non-CpG promoters more frequently had lower basal

126 levels (i.e. levels at 0h, before stimulation) of activation-associated histone modifications, such as

127 H3K27ac, H3K9K14ac, H3K4me3, and similarly lower levels of Pol2 binding and pre-stimulation gene

128 expression (Fig. S2B). This partly explains the higher frequency of significant increases in histone

129 modifications at LPS-induced promoters (Fig. S2B), and the higher fold-induction of genes associated

130 with non-CpG promoters (Fig. S2C).

131 Previous studies have reported only limited combinatorial complexity between histone  
132 modifications, i.e. subsets of modifications are highly correlated in their occurrence [27,28]. In our  
133 data too, basal levels of activation markers at promoters and, to a lesser degree at enhancers, were  
134 highly correlation (Fig. S3). Stimulus-induced accumulations of histone modifications and Pol2  
135 binding at promoters and enhancers further support this view. For example, increases in H3K9K14ac,  
136 H3K4me3, H3K36me3, H3K27ac, Pol2 binding, and transcription often occurred at the same  
137 promoters (Fig. 1D). Similarly, increases in H3K9K14ac, H3K27ac, Pol2 binding, and transcription  
138 often coincided at enhancer regions (Fig. 1E). In general, activated regions experienced increases in  
139 several activation markers.

#### 140 [Several Histone Modifications are Induced at a Specific Time after Stimulation](#)

141 Focusing on the set of induced promoters, we analyzed the ordering of induction times of different  
142 features (transcription activity, Pol2 binding, histone modifications). We defined the “induction time”  
143 of a feature  $X$  in a genomic locus as the first time point (if any) where  $X$  was increased significantly  
144 compared to its basal level in that loci (i.e. at 0h; see Methods). Defining induction times in  
145 individual genomic loci is not straightforward, due to the noisy nature of biological data. Therefore,  
146 we here focused on genome-wide trends by analyzing induction times in sets of promoters and  
147 enhancers.

148 As a proof of concept and a positive control, we observed that RNA reads (based on RNA-seq)  
149 mapped to promoter regions were generally induced at the same time and in the same order of the  
150 induction of transcription initiation (based on TSS-seq, independent of RNA-seq data; Fig. 2A (top)  
151 and Fig. S4). E.g. at promoters with early induction of transcription initiation (TSS-seq) there was an  
152 early induction of mapped RNA reads, while those with later induction have later induction of  
153 mapped RNA reads. Plotting the same data using cumulative plots, we again observed that increases  
154 in RNA-seq reads roughly follow the same order as transcription induction times (Fig. 2A, bottom).

155 Promoters of stably expressed genes lack induction of mapped RNA reads at their promoter. Similar  
156 observations were made for induction of Pol2 binding (Fig. 2B).

157 However, in striking contrast, induction times of H3K9K14ac, H3K4me3, and H3K36me3 at LPS-  
158 induced promoters were concentrated within specific time windows (Fig. 2D-F), and, moreover, the  
159 time of induction of these markers appeared to be largely independent of transcriptional induction  
160 times. Induction of H3K9K14ac was in general concentrated between 0.5h and 3h after stimulation  
161 (Fig. 2D), although promoters with early induction of transcription (0.5h, 1h, 2h) tended to have  
162 early increases in H3K9K14ac (at 0.5h). Even genes with transcriptional induction at 3, 4h (and to a  
163 lesser extend 6 and 8h) had induction of H3K9K14ac mostly before 3h after stimulation. Therefore,  
164 the induction of acetylation for these promoters *preceded* induction of transcription. Very few  
165 promoters showed significant increases later than 3 hours after stimulation. Finally, at promoters  
166 with late induction (16h, 24h) or at stably active promoters, increases in H3K9K14ac were rare (not  
167 shown in Fig. 2 in the interest of clarity).

168 In contrast with H3K9K14ac, no significant induction of H3K4me3 was observed at time points 0.5h  
169 and 1h (Fig. 2E). Induction of H3K4me3 at LPS-induced promoters was concentrated between 2 and  
170 4 hours after stimulation, regardless of their transcriptional induction times. While induction of  
171 H3K4me3 was rare at immediate-early promoters, between 20 to 45% of promoters induced at 1h,  
172 2h, 3h, 4h, 6h, and 8h had significant increases of this modification. These results suggest that  
173 stimulus-induced accumulation of H3K4me3 is not necessarily a prerequisite nor a direct  
174 consequence of transcription induction, since it can both *precede* or *follow* induction of transcription  
175 (see also Discussion).

176 Finally, H3K36me3 was only induced at later time points, especially at 16h and 24h, regardless of  
177 transcriptional induction times of promoters (Fig. 2F). In contrast with H3K9K14ac and H3K4me3,  
178 H3K36me3 is located within gene bodies and peaks towards their 3' end (Fig. S5) [29]. Upon  
179 stimulation, H3K36me3 gradually accumulated within the gene bodies of LPS-induced genes,



180 spreading towards the 5' end, and reached the promoter region at the later time points in our time  
181 series (Fig. S5A). Stably expressed genes had on average high basal levels of H3K36me3, with only  
182 limited changes over time. However, interestingly, at time points 16-24h, an accumulation of  
183 H3K36me3 was observed towards their 5' end (Fig. S5B), resulting in a relatively high fraction of  
184 stably expressed promoters having an induction of H3K36me3 (6.9%). Induction of H3K9me3 was  
185 rare at promoters, but this too had a tendency to occur at later time points (16h and 24h; Fig. S6A).

186 Remarkably, the induction times of H3K9K14ac, H3K4me3, and H3K36me3 at promoters did not  
187 change depending on their basal levels (Fig. S7); regardless of their pre-stimulus levels, increases in  
188 H3K9K14ac were early, followed by H3K4me3, and H3K36me3 accumulation was late. This might  
189 indicate that a common mechanism is regulating these accumulations, regardless of basal levels.

190 The tendencies described above were confirmed using RT-qPCR and ChIP-qPCR measuring RNA,  
191 H3K9K14ac, H3K4me3 (see WT data in Fig. 7), and H3K36me3 (Fig. S8) at the promoters of 9 LPS-  
192 induced genes. In general, accumulation of H3K9K14ac in WT occurred before that of H3K4me3, and  
193 accumulation of H3K36me3 was late.

194 Significant increases in H3K27ac appeared to be relatively rare at promoters (Fig. 2C), and were  
195 somewhat enriched at earlier time points (0.5h, 1h, and 2h). However, promoters with later  
196 induction of transcription experienced later accumulation of H3K27ac. The pattern for H3K27ac  
197 therefore appeared to be an intermediate between that of H3K9K14ac (early increases), and that of  
198 RNA or Pol2 (increases follow transcription induction times). Very few inductions were observed for  
199 H3K27me3 and H3K4me1 (Fig. S6B-C).

200 Increases in histone modifications were more frequent at non-CpG promoters than at CpG island-  
201 associated promoters (Fig. S9). This can be explained by the lower basal levels of most activation-  
202 associated histone modifications at non-CpG promoters (Fig. S2B). However, no differences in the  
203 accumulation times were observed between both types of promoters.

## 204 Similarities and Differences between Enhancer and Promoter Induction Patterns

205 Interactions between enhancers and promoters could allow active histone modifiers at promoters to  
206 also affect modifications at enhancer regions, and vice versa. We therefore analyzed induction of  
207 features at enhancers in function of induction of transcription at promoters.

208 To some degree, we found similar tendencies at enhancers assigned to induced promoters. We  
209 found that a small fraction of RNA-seq reads was aligned to enhancers, indicating that polyA-tailed  
210 enhancer-associated transcripts were transcribed from these regions. Induction of enhancer-  
211 associated transcripts to some extent followed the order of transcription induction at nearby  
212 promoters, though they seemed to somewhat precede transcription induction at promoters, and  
213 increases were relatively frequent at early time points (0.5 and 1h; Fig. 3A). These observations fit  
214 with those reported in a recent study showing that transcription at enhancers precedes that of  
215 promoters in cells treated with various stimuli [30]. We observed a somewhat similar, though  
216 weaker, pattern for Pol2 binding at enhancers (Fig. 3B).

217 For H3K9K14ac, the induction pattern at enhancers was similar to that observed for promoters (Fig.  
218 3C); induction of H3K9K14ac was mainly concentrated at time points 2h and 3h after stimulation.  
219 Although in general a lower percentage of enhancers experienced increases of H3K9K14ac than  
220 promoters (5-10% vs 20-50%), typically 20-40% of induced promoters had at least one assigned  
221 enhancer at which an induction of H3K9K14ac occurred (Fig. S10). Increases in H3K27ac at enhancers  
222 appeared to follow to some degree the order of transcription induction of nearby promoters (Fig.  
223 3D), in a pattern that was more similar to that of Pol2 and RNA-seq reads.

224 Finally, for other modifications, there are discrepancies between promoters and enhancers. We  
225 observed a gradual increase in H3K4me1 markers at enhancers over the time course (Fig. S11A), and  
226 limited increases in H3K36me3 (Fig. S11B), again independent of timing of transcriptional induction.  
227 H3K4me3, H3K9me3, and H3K27me3 signals were in general low, and no increases were observed  
228 (Fig. S11C-E).

## 229 Correlation between LPS-induced TF Binding and Increases in Epigenetic Features

230 Next, to reveal potential regulatory mechanisms underlying the epigenetic changes induced by LPS,  
231 we performed an integrative analysis of our histone modification data with TF binding data. For this  
232 we used a publicly available ChIP-seq dataset for 24 TFs with high expression in mouse DCs [25],  
233 before and after treatment with LPS (typical time points include 0h, 0.5h, 1h, and 2h, see Methods).

234 As reported in the original study, we observed widespread pre-stimulation binding of both stably-  
235 expressed and LPS-induced promoters by PU.1 and C/EBP $\beta$ , and to a lesser degree by IRF4, JUNB,  
236 and ATF3 [25] (Fig. S12A). The known association between H3K4me1 and binding by PU.1 and  
237 C/EBP $\beta$  was also successfully recapitulated (Fig. S13A,B) [10,13]. Binding by TFs controlling the  
238 response to LPS, such as NF- $\kappa$ B (subunits NFKB1, REL, and RELA) and STAT family members, was  
239 relatively frequent at LPS-induced promoters (Fig. S12B).

240 Focusing on the overlap between LPS-induced TF binding at promoters and enhancers, and induction  
241 of epigenetic features, we found that new binding of promoters by RelA, IRF1, STAT1, and STAT2 was  
242 especially associated with increases in H3K9K14ac, H3K4me3, H3K36me3, transcription, and to a  
243 lesser degree Pol2 binding and H3K27ac (Fig. 4; Fisher's exact test). For example, of the 418  
244 promoter regions that become newly bound by STAT1 after stimulation, 223 (53.3%) experience  
245 increases in H3K9K14ac (vs 3.0% of promoters not bound by STAT1; p: 8.3E-205). LPS-induced  
246 binding by the same four TFs was also strongly associated with increases in H3K9K14ac and H3K27ac  
247 at enhancers (Fig. 4). Combinations of these four TFs often bind to the same promoter and enhancer  
248 regions (Fig. S12C,D), and STAT1 functions both as a homodimer or as a heterodimer with STAT2 [31].  
249 LPS-induced TFs, including NF- $\kappa$ B and STAT family members, have been shown to bind preferentially  
250 at loci that are pre-bound by PU.1, C/EBP $\beta$ , IRF4, JUNB, and ATF3 [25]. Accordingly, histone  
251 modifications were also more frequently observed at regions that were pre-bound by these five TFs  
252 (Fig. S14).

253 Weaker associations were found for LPS-induced binding by other NF- $\kappa$ B subunits (NFKB1, REL, and  
254 RELB), TFs that are widely active even before stimulation (C/EBP $\beta$ , ATF3, JUNB, and IRF4), and E2F1,  
255 which has been shown to be recruited by NF- $\kappa$ B through interaction with Rela [32].

256 Together, these results suggests a strong correlation between increases in activation marker histone  
257 modifications and LPS-induced binding by RelA, IRF1, STAT1 and STAT2.

### 258 STAT1 and STAT2 Binding Coincides with Accumulation of H3K9K14ac, and Precedes 259 Accumulation of H3K4me3

260 The relative timing of LPS-induced TF binding events and increases in histone modifications can  
261 reflect potential causal relationships. As described above, H3K9K14ac levels increase mainly during  
262 the first 3 hours after LPS stimulation (Fig. 2D). Particularly, many LPS-induced promoters show  
263 increases in H3K9K14ac between 2 and 3 hours after stimulation, and we found a strong overlap  
264 between increases in H3K9K14ac and binding by STAT1 (Fig. 4). STAT1 is not active before  
265 stimulation, and its activity is only induced about 2 hours after LPS stimulation [33], resulting in a  
266 strong increase in STAT1-bound loci (from 56 STAT1-bound loci at 0h to 1,740 loci at 2h; Fig. S12B).

267 We observed a particularly strong coincidence in timing between STAT1 binding and increases in  
268 H3K9K14ac (Fig. 5A): genomic regions that become bound by STAT1 at 2h show a coinciding sharp  
269 increase in H3K9K14ac around the STAT1 binding sites. At promoters and enhancers that became  
270 bound by STAT1 at 2h the induction of H3K9K14ac was particularly frequent (Fig. 5B,C). At the 2 hour  
271 time point, STAT1 binds 378 enhancers and 409 promoters, and at the same time there is a  
272 widespread induction of H3K9K14ac at these target regions (Fig. 5B,C). Accumulation of H3K9K14ac  
273 was very rare at these regions before STAT1 binding. At the end of our time series, 222 (54.2%) of  
274 these promoters, and 214 (56.6%) of these enhancers, had significantly increased H3K9K14ac levels  
275 (versus only 3.0% of promoters and 3.3% of enhancers lacking STAT1 binding).

276 Similar to H3K9K14ac, we observed a general increase in H3K4me3 around STAT1 binding sites (Fig.  
277 5D). However, in contrast with H3K9K14ac, STAT1 binding immediately precedes the induction of  
278 H3K4me3 (between 2-4 hours). Accordingly, only 21 STAT1-bound promoters (out of 409; 5.6%) had  
279 significant increases at 2 h, but an additional 111 promoters (27.1%) experienced increases at the  
280 following time points (3-4 hours; Fig. 5E). As noted above, H3K4me3 was in general absent at  
281 enhancers.

282 Similar patterns were observed for enhancers and promoters bound by STAT2 2 hours after  
283 stimulation (Fig. S15). In contrast, regions bound by RelA and IRF1 showed increased levels of  
284 H3K27ac and to a lesser degree H3K9K14ac at earlier time points (Fig. S16 and S17). Associations  
285 with H3K9K14ac induction after 2 hours were weak compared to STAT1/2. Average increases in  
286 H3K4me3 at RelA- and IRF1-bound regions were only modest (Fig. S16G-I and S17G-I), suggesting  
287 that the association between RelA- and IRF1-binding and H3K4me3 as seen in Fig. 4 is mostly  
288 through co-binding at STAT1/2-bound regions. Associations between histone modifications and  
289 binding by other TFs were in general weak (not shown; see also Fig. 4). No changes were observed in  
290 H3K4me1 at STAT1/2-bound regions (Fig. S18A). Although there was a tendency for STAT1/2-bound  
291 loci to have increases in H3K27ac, binding seemed to slightly lag behind H3K27ac induction (Fig.  
292 S18B). Finally, although STAT1/2-bound regions tended to experience increases in H3K36me3, the  
293 time lag between binding and induction was large (Fig. S18C). This is also true for other TFs, such as  
294 RelA and IRF1, and even PU.1 and C/EBP $\beta$ , regardless of the timing of TF binding (Fig. S13C-F).

295 These results suggest possible causal relationships between STAT1/2 binding and the accumulation  
296 of H3K9K14ac and H3K4me3. The specific timing of increases in these modifications might reflect the  
297 timing of activation of these TFs, resulting in the recruitment of acetyl transferases and methyl  
298 transferases to specific promoter and enhancer regions.

299 LPS-induced Accumulation of H3K9K14ac and H3K4me3 is especially frequent at  
300 STAT1/2-bound Promoters of TRIF-dependent Genes

301 In *Trif*<sup>-/-</sup> cells, LPS-induced type I IFN production, activation of the JAK-STAT pathway, and induction  
302 of STAT1 and STAT2 target genes are severely impaired. Under the hypothesis that there is a causal  
303 relation between STAT1/2 binding and induction of H3K9K14ac and/or H3K4me3, we would  
304 therefore expect an especially high overlap between genes with decreased expression in *Trif*<sup>-/-</sup> cells,  
305 and promoters with induction of H3K9K14ac or H3K4me3 following stimulation in the WT. On the  
306 other hand, MyD88-dependent but TRIF-independent genes should mostly lack STAT1 and STAT2  
307 binding, and are therefore expected to lack induction of these modifications.

308 Using RNA-seq data from LPS-stimulated *Myd88*<sup>-/-</sup> and *Trif*<sup>-/-</sup> cells, we defined a set of 141 TRIF-  
309 dependent genes (Fig. 6A). These genes typically have induction around 3-6 hours after stimulation  
310 in WT and *Myd88*<sup>-/-</sup>, but lack induction of transcription in the *Trif*<sup>-/-</sup> cells. We found that a high  
311 fraction of the TRIF-dependent genes were bound by STAT1 and STAT2 in the WT ChIP-seq samples 2  
312 hours after stimulation (STAT1: 64.5%, STAT2: 57.4%; compare: MyD88-dependent genes: 10.6% and  
313 9.1%; Fig. 6B). This suggests that these genes are indeed under the control of STAT1 and/or STAT2 in  
314 WT.

315 Within these 141 TRIF-dependent genes, 97 (68.8%) had increases in H3K9K14ac at time points 2-3  
316 hours (Fig. 6C). After dividing these TRIF-dependent genes by presence or absence of STAT1/2  
317 binding, a clear difference in H3K9K14ac induction was observed: 81 out of 91 (89.0%) TRIF-  
318 dependent STAT1-bound genes, and 75 out of 81 (92.6%) of TRIF-dependent STAT2-bound genes  
319 had induction of H3K9K14ac between 2-3 hours. In contrast, only 13 out of 47 (27.7%) of TRIF-  
320 dependent genes lacking binding by STAT1 and STAT2 had induction of H3K9K14ac. As a reference,  
321 only 11 out of 66 (16.7%) of MyD88-dependent genes had H3K9K14ac induction at these time points.

322 A similar tendency was observed for H3K4me3 induction at time points 2-4h (Fig. 6D). 78 (55.3%) of  
323 TRIF-dependent genes had increases in H3K4me3 at time points 2-4 hours. Only 10 out of 47 (21.3%)

324 TRIF-dependent genes lacking STAT1 and STAT2 binding, and only 10 out of 66 (15.2%) MyD88-  
325 dependent genes had induction of H3K4me3 at these time points. In contrast, 66 (72.5%) of STAT1-  
326 bound, and 62 (76.5%) of STAT2-bound promoters had increases.

327 [A Subset of STAT1/2 Target Genes lack Induction of H3K9K14ac and H3K4me3 in \*Trif\*<sup>-/-</sup>,](#)  
328  [\*Irf3\*<sup>-/-</sup>, and \*Ifnar1\*<sup>-/-</sup> cells](#)

329 We further analyzed the roles of the TRIF-dependent signaling pathway and STAT1/2 in regulating  
330 LPS-induced genes, using RT-qPCR and CHIP-qPCR in WT, *Trif*<sup>-/-</sup>, *Irf3*<sup>-/-</sup>, and *Ifnar1*<sup>-/-</sup> cells. Experiments  
331 were performed on a selection of known TRIF-dependent and TRIF-independent genes, which  
332 showed increases in H3K9K14ac and H3K4me3 in WT (Fig. 7).

333 A set of known TRIF-independent genes (*Tnf*, *Il1b*, *Cxcl1*, and *Nfkbiz*) had no change between WT and  
334 knock outs (KOs) in the induction of gene expression, H3K9K14ac and H3K4me3 (Fig. 7A). These  
335 genes are not bound by STAT1/2 (except for *Cxcl1* which is bound only by STAT2), and the induction  
336 of histone modifications at their promoter regions is likely to be STAT1/2-independent.

337 A second subset of LPS-induced genes (*Ifit1* and *Rsad2*) has TRIF-dependent expression. These genes  
338 become bound by STAT1/2 2 hours after LPS stimulation. Their expression and the induction of  
339 H3K9K14ac and H3K4me3 were completely abrogated in *Trif*<sup>-/-</sup> cells, in *Irf3*<sup>-/-</sup> cells, and in *Ifnar1*<sup>-/-</sup> cells  
340 (Fig. 7B). These results further support a role of STAT1 and/or STAT2 in the control of chromatin  
341 modifications at the promoters of these genes.

342 A third subset of genes (*Cxcl10*, *Ccl5*, and *Il6*) was partially dependent on TRIF, IRF3, and IFNR in their  
343 induction of gene expression and histone modification changes (Fig. 7C). Induction of H3K4me3 was  
344 abrogated for *Cxcl10* in all three KOs, although H3K9K14ac was only affected in *Trif*<sup>-/-</sup> cells.  
345 Modifications at *Ccl5* and *Il6* too, showed a dependency of TRIF, but not on IFNR. Although these  
346 three genes were bound by STAT1 or STAT2 2 hours after LPS stimulation, it is likely that their gene  
347 expression and histone modifications are regulated by additional, partly redundant signaling

348 pathways downstream of TLR4 [34]. Indeed, RelA and IRF1 bind to the promoters of these genes,  
349 supporting the notion of combinatorial control of gene expression and histone modifications.

350 Furthermore, stimulation of WT cells using IFN- $\beta$  induced expression of *Ifit1* and *Rsad2*, and  
351 accumulation of H3K9K14ac and H3K4me3 at their promoters (Fig. S19B). In this system, the  
352 activation of the IFNR signaling pathway, and of STAT1/2, is independent of TRIF. Accordingly, this  
353 accumulation of H3K9K14ac and H3K4me3 was not affected in *Trif*<sup>-/-</sup> cells, further supporting a role  
354 for STAT1/2 in the control of these modifications at these genes. Similar accumulations were  
355 observed for *Cxcl10*, *Ccl5*, and *Il6* (Fig. S19C). Although the resolution of the data is not enough to  
356 make a definite statement, accumulation of H3K9K14ac following IFN- $\beta$  stimulation had a tendency  
357 to start earlier at several of these five promoters in both WT and *Trif*<sup>-/-</sup> cells, compared to LPS-  
358 stimulated cells, possibly reflecting a faster activation of STAT1/2. In contrast, no or only limited  
359 accumulation was not observed for *Tnf*, *Il1b*, *Cxcl1*, and *Nfkbiz* (Fig. S19A).

## 360 Discussion

361 The concept of active genes being in an open chromatin conformation was introduced several  
362 decades ago [35], yet the contribution of histone modifications to the control of gene activity  
363 remains controversial [15]. On the other hand, the contribution of TFs to regulating gene expression  
364 is widely recognized [36], and a few studies have identified crosstalk between TFs and histone  
365 modifiers as important in the regulation of the response to immune stimuli. Induction of enhancer  
366 histone modifications was found to be associated with LPS stimulation-induced gene expression [7].  
367 I $\kappa$ B $\zeta$  was shown to control gene expression of *Lcn2* and *Il12b* as well as H3K4me3 in their promoters  
368 [37]. This process further induces recruitment of the SWI/SNF chromatin remodeling complex,  
369 which is regulated by Akirin2 [38]. Histone modifications such as deacetylation by histone  
370 deacetylases [39] and H3K9me3 demethylation by Jmjd2d [40], have been linked to the induction of  
371 a small set of genes upon LPS stimulation. Nevertheless, our understanding about causal



372 relationships between TF binding, changes in histone modifications, and changes in transcriptional  
373 activity of genes in response to stimuli is still lacking.

374 Analysis of the ordering of events over time can reveal insights into possible causal relationships or  
375 independence between them. Here, we presented an integrative study of the timing and ordering of  
376 changes in histone modifications, in function of transcriptional induction in response to an immune  
377 stimulus. Our results suggest that, rather than a clear temporal order between stimulus-induced  
378 chromatin remodeling followed by transcriptional activation, specific histone modifications appear  
379 to be induced at specific time frames after stimulation. These time frames appear to be relatively  
380 independent of the timing of induction of transcription.

381 In our dataset, we roughly observed three “waves” of modifications. The first was early induction of  
382 H3K9K14ac, which occurs mainly in the first three hours after stimulation. Here, we did observe that  
383 some immediate-early promoters tended to have immediate induction of acetylation. However,  
384 changes were concentrated at time points 2h and 3h. A second wave consisted of H3K4me3,  
385 occurring mainly at 2-4 hours following stimulation. For genes with early transcriptional induction,  
386 this modification therefore only occurs *after* induction of transcription, while it *precedes* induction of  
387 transcription for genes with later induction times. Although H3K4me3 is widely used as a marker for  
388 active genes, the functional role of this modification is still unclear. For example, the deletion of Set1,  
389 the only H3K4 methyltransferase in yeast, resulted in slower growth than in wild type, but otherwise  
390 appears to have only limited effects on transcription [17]. Other studies too have reported a lack of a  
391 direct effect of H3K4me3 on transcription [18,19]. Another study showed that H3K4  
392 methyltransferase Wbp7/MLL4 controls expression of only a small fraction of genes directly [41].  
393 Together, these and our results hint at a lack of a causal relationship between transcription and  
394 H3K4me3 on a genome-wide scale. Finally, a third and last wave consisted of changes in H3K36me3  
395 and H3K9me3, occurring only around 16-24 hours after stimulation. On the other hand, induction of  
396 H3K27ac was not limited to a specific time frame, but was more correlated with transcription

397 induction times. Interestingly, fluorescence microscopy experiments have shown that H3K27ac  
398 levels, and not H3K4me3, can alter Pol2 kinetics by up to 50% [19]. The induction time patterns of  
399 histone modifications could therefore indeed present hints about active or passive roles of different  
400 histone modifications.

401 Since the induction of remodeling appears to occur specifically at LPS-induced genes, it is likely that  
402 histone modifiers are recruited by one or more LPS-activated TFs to specific target regions in the  
403 genome defined by the binding specificity of the TFs. In this scenario, the timing of activation of the  
404 TFs could explain the “waves” of histone modification changes. This fits well with our observations  
405 for STAT1/2 and the induction of H3K9K14ac and H3K4me3, within specific time frames and mostly  
406 restricted to LPS-induced promoters. Other studies have reported associations between STAT1  
407 binding and changes in epigenetic markers following environmental stimulation, including the  
408 activation of latent enhancers [7] and histone acetylation [39,42]. Moreover, epigenetic priming by  
409 histone acetylation through STAT1 binding to promoters and enhancers of *Tnf*, *Il6*, and *Il12b* has  
410 been reported [43]. Interestingly, these genes lack canonical STAT1 binding sites, and the acetylation  
411 at these genes did not directly result in transcriptional induction, but enhanced TF and Pol2  
412 recruitment after subsequent TLR4 activation. Since TFs such as STAT1 are also known to induce  
413 gene expression, one might expect induction of histone modifications to co-occur with induction of  
414 expression. However, as we described here, and as supported by the above studies, this is not  
415 necessarily the case. Gene expression is known to be regulated by combinations of TFs, and in this  
416 study too we noticed that LPS-activated TFs such as NF- $\kappa$ B, IRF1 and STATs often bound to the same  
417 loci (Fig. S12), which were moreover often pre-bound by several other TFs, including PU.1 and  
418 C/EBP $\beta$ . Discrepancies between timing of expression induction and accumulation of histone  
419 modifications could be caused by different requirements for combinatorial binding. This could also  
420 explain widely-reported “non-functional” TF binding, where TF binding does not seem to affect the  
421 activity of nearby genes [44]. Such “non-functional” TF binding might instead trigger changes in  
422 histone modifications that remain unnoticed and affect gene activity in more subtle ways.

423 Although many studies have compared histone modifications before and after stimulation, most lack  
424 sufficient time points and resolution to allow analysis of temporal ordering of changes. One recent  
425 study in yeast reported results that are partly similar to ours [45]: specific modifications (especially,  
426 but not only, acetylation) occur at earlier time frames during the response of yeast to diamide stress,  
427 and others at later time points. Interestingly, even late changes in histone modifications in yeast  
428 (including H3K36me3) were reported to occur within just one hour after stimulation. In contrast,  
429 changes in H3K36me3 in our data were concentrated between 16-24 hours after stimulation. Thus,  
430 the time scales of stimulus-induced epigenetic changes in multicellular, higher mammalian systems  
431 might be much longer. Interestingly, increases in H3K36me3 around 16-24 h often coincide with a  
432 decrease in histone acetylation towards pre-stimulation levels at LPS-induced promoters. A study in  
433 yeast suggested that H3K36me3 plays a role in the activation of a histone deacetylase [46], and  
434 might therefore play a role in the return to a basal state of histone modifications and terminating  
435 the response to stimulus.

## 436 Conclusions

437 Our time series ChIP-seq data and analysis present a first genome-wide view of the timing and order  
438 of accumulation of histone modifications during a stress response in mammalian immune cells. The  
439 stimulus-induced accumulation of H3K9K14ac and H3K4me3 occurred within specific time frames,  
440 and appears to be independent of transcriptional induction times. Integrative analysis suggests a  
441 role for STAT1/2 in the induction of these markers at stimulus-dependent promoters and enhancers.  
442 Together these findings hint at the absence of direct causal relationship between these histone  
443 modifications and transcription. Stimulus-induced changes in modifications more likely reflect the  
444 activation of stimulus-dependent TFs and their interactions with chromatin modifiers.

## 445 Material and Methods

### 446 Reagents, cells, and mice

447 Bone marrow cells were prepared from C57BL/6 female mice, and were cultured in RPMI 1640  
448 supplemented with 10 % of fetal bovine serum under the presence of murine granulocyte/monocyte  
449 colony stimulating factor (GM-CSF, purchased from Peprotech) at the concentration of 10 ng/mL.  
450 Floating cells were harvested as bone marrow-derived dendritic cells (BM-DCs) after 6 days of  
451 culture with changing medium every 2 days. The cells were stimulated with LPS (Salmonella  
452 minnesota Re595, purchased from Sigma) at the concentration of 100 ng/mL for 0, 0.5, 1, 2, 3, 4, 6,  
453 8, 16, and 24 hours, and were subjected to RNA extraction or fixation. Murine IFN- $\beta$  was purchased  
454 from Pestka Biomedical Laboratories, and was used to stimulate the cells at the concentration of  
455  $1 \times 10^2$  unit/mL. All animal experiments were approved by the Animal Care and Use Committee of  
456 the Research Institute for Microbial Diseases, Osaka University, Japan (IFReC-AP-H26-0-1-0). TRIF-,  
457 IRF3-, or IFNR-deficient mice have been described previously [47–49].

### 458 ChIP-seq experiments

459 For each time point, thirty million BM-DCs were stimulated with LPS and subjected to fixation with  
460 addition of 1/10 volume of fixation buffer (11% formaldehyde, 50 mM HEPES pH 7.3, 100 mM NaCl,  
461 1 mM EDTA pH 8.0, 0.5 mM EGTA pH8.0). The cells were fixed for 10 minutes at room temperature,  
462 and immediately washed with PBS three times. ChIP and sequencing were performed as described  
463 (Kanai et al, DNA Res, 2011). Fifty microliter of lysate after sonication was aliquoted as “whole cell  
464 extract” (WCE) control for each IP sample. Antibodies used were Pol2 (05-623, Millipore), H3K4me3  
465 (ab1012, Abcam), H3K9K14ac (06-599, Millipore), H3K36me3 (ab9050, Abcam), H3K9me3 (ab8898,  
466 Abcam), H3K27me3 (07-449, Millipore), H3K4me1 (ab8895, Abcam), and H3K27ac (ab4729, Abcam).

#### 467 RNA extraction and RT-qPCR.

468 One million BM-DCs were stimulated with LPS for indicated times and subjected to RNA extraction  
469 by using TRIzol (Invitrogen) according to manufacturer's instruction. RNAs were reverse transcribed  
470 by using RevaTra Ace (Toyobo). The resulting cDNAs were used for qPCR by using Thunderbird SYBR  
471 master mix (Toyobo) and custom primer sets (Table S1). QPCR was performed by using LightCycler  
472 Nano (Roche).

#### 473 ChIP-qPCR

474 ChIP was done as above, except  $4 \times 10^6$  cells were used. The resulting ChIP-DNAs were subjected to  
475 qPCR as same as RT-qPCR, using custom primer sets (Table S2).

#### 476 Peak calling and processing of ChIP-seq data

477 For each histone modification and for Pol2 binding data, we aligned reads to the genome, conducted  
478 peak calling and further processing as follows.

479 We mapped sequenced reads of ChIP-seq IP and control (WCE) samples using Bowtie2 (version  
480 2.0.2), using the parameter "very-sensitive", against the mm10 version of the mouse genome [50].  
481 Processing of alignment results, including filtering out low MAPQ alignments (MAPQ score < 30) was  
482 performed using samtools [51].

483 We predicted peaks for each time point using MACS (version 1.4.2) [52], using each IP sample as  
484 input and its corresponding WCE sample as control. To improve the detection of both narrow and  
485 broad peaks, peak calling was performed using default settings and also using the "nomodel"  
486 parameter with "shiftsize" set to 73. Negative control peaks were also predicted in the control  
487 sample using the IP sample as reference. Using the predicted peaks and negative control peaks, we  
488 set a threshold score corresponding to a false discovery rate (FDR) of 0.01 (number of negative  
489 control peaks vs true peaks), for each time point separately. All genomic regions with predicted  
490 peaks were collected over all 10 time points, and overlapping peak regions between time points

491 were merged together. Moreover, we merged together peak regions separated by less than 500 bps.  
492 This gave us a collection of all genomic regions associated with a peak region in at least one sample  
493 of the time series.

494 In a next step, we counted the number of reads mapped to each region at each time point for both  
495 the IP samples and WCE control samples. Using these counts, we performed a read count correction,  
496 as described by Lee et al. [53]. Briefly, this method subtracts from the number of IP sample reads  
497 aligned to each peak region the expected number of non-specific reads given the number of reads  
498 aligned to the region in the corresponding WCE sample. The resulting corrected read count is an  
499 estimate of the number of IP reads in a region that would remain if no WCE reads are present [53].  
500 This correction is necessary for the quantitative comparison of ChIP signals over time in the  
501 downstream analysis.

502 Finally, the corrected read counts were converted to reads per kilobase per million reads (RPKM)  
503 values (using read counts and the lengths of each region), and normalized using quantile  
504 normalization, under the assumption that their genome-wide distribution does not change  
505 substantially during each time series. The normalized RPKM values were converted to reads per  
506 million read (ppm) values.

### 507 TSS-seq data processing and promoter definition

508 TSS-seq data for BM-DCs before and after stimulation with LPS was obtained from the study by Liang  
509 *et al.* [22] (DDBJ accession number DRA001234). TSS-seq data reflects transcriptional activity, but  
510 also allows for the detection of TSSs on a genome-wide scale at a 1 base resolution [54]. Mapping of  
511 TSS-seq samples was done using Bowtie2, as for ChIP-seq data. The location (5' base) of the  
512 alignment of TSS-seq reads to the genome indicates the nucleotide at which transcription was  
513 started. In many promoters, transcription is initiated preferably at one or a few bases. Because of  
514 this particular distribution of TSS-seq reads mapped to the genome, default peak calling approaches

515 cannot be applied. Instead, we used the following scanning window approach for defining regions  
516 with significantly high number of aligned TSS-seq reads.

517 The number of TSS-seq reads mapped to the genome in windows of size 1, 10, 50, 100, 500, and  
518 1000 bases were counted in a strand-specific way, in steps of 1, 1, 5, 10, 50, and 100 bases. As a  
519 control, a large number of sequences was randomly selected from the mouse genome, and mapped  
520 using the same strategy, until an identical number of alignments as in the true data was obtained.  
521 For these random regions too, the number of reads was counted using the same scanning window  
522 approach. The distribution of actual read counts and control read counts were used to define a FDR-  
523 based threshold (FDR: 0.001) for each window size. For overlapping regions with significantly high  
524 read counts, the region with the lowest associated FDR was retained.

525 In order to remove potentially noisy TSSs, we removed TSSs that were located within 3' UTRs, and  
526 TSSs located >50 kb upstream of any known gene. For remaining TSSs, we used a simple model (see  
527 Supplementary material) 1) to decide the representative TSS location in case a promoter region  
528 contained several candidate main TSSs, 2) to remove TSS-seq hits lacking typical features of  
529 promoters (e.g. presence of only TSS-seq reads in absence of histone modifications and Pol2 binding),  
530 and 3) to decide the main promoter of a gene in case there were multiple candidates. Finally, we  
531 obtained 9,964 remaining high-confidence TSSs, each assigned to 1 single Refseq gene.

532 These TSS-seq-based TSSs were supplemented with 14,453 non-overlapping Refseq-based TSSs for  
533 all Refseq genes which did not have an assigned high-confidence TSS-seq-based TSS. Most of the  
534 genes associated with these TSSs had lower expression in our RNA-seq data (mostly RPKM is 0 or < 1;  
535 not shown). Together, TSS-seq-based TSSs and Refseq-based TSSs resulted in a total of 24,416  
536 promoter regions.

537 CpG-associated promoters were defined as those having a predicted CpG island (from the UCSC  
538 Genome Browser Database) in the region -1kb to +1kb surrounding the TSS [55]. Other promoters  
539 were considered to be non-CpG promoters.

## 540 Definition of enhancers

541 Enhancers were defined based on the signals of H3K4me1 and H3K4me3. First, we collected all  
542 genomic regions with significantly high levels of H3K4me1 (see section “Peak calling and processing  
543 of ChIP-seq data”) in at least one of the ten time points. Regions located proximally (<2kb distance)  
544 to promoter regions and exons were removed, because they are likely to be weak H3K4me1 peaks  
545 observed around promoters, as were H3K4me1-positive regions of excessively large size (>10kb).  
546 Finally, we removed regions with  $H3K4me1 < H3K4me3 * 5$ , resulting in 34,072 remaining enhancers.  
547 Enhancers were naively assigned to the nearest promoter (TSS-seq based or Refseq-based) that was  
548 < 150kb separated from it (center-to-center). For 30,448 enhancers (89%) a promoter could be  
549 assigned.

## 550 Public ChIP-seq data for TFs

551 Genome-wide binding data (ChIP-seq) is available for mouse DCs before and after stimulation with  
552 LPS, for a set of 24 TFs with a known role of importance and/or high expression in DCs [25] (GEO  
553 accession number GSE36104). TFs (or TF subunits) included in this dataset are Ahr, ATF3, C/EBP $\beta$ ,  
554 CTCF, E2F1, E2F4, EGR1, EGR2, ETS2, HIF1a, IRF1, IRF2, IRF4, JUNB, MafF, NFKB1, PU.1, Rel, RelA,  
555 RelB, RUNX1, STAT1, STAT2, and STAT3. Typically time points in this data are 0h, 0.5h, 1h, and 2h  
556 following LPS stimulation (some TFs lack one or more time points). We used the ChIP-seq-based  
557 peak scores and score threshold as provided by the original study as an indicator of significant TF  
558 binding.

559 Promoters (region -1kb to +1kb around TSS) and enhancers (entire enhancer region or region -1kb to  
560 +1kb around the enhancer center for enhancers < 2 kb in size) were considered to be bound by a TF  
561 if they overlapped a ChIP-seq peak with a significantly high peak score. New binding events by a TF  
562 at a region were defined as time points with a significantly high score where all previous time points  
563 lacked significant binding.



## 564 Definition of induction of histone modifications and Pol2 binding

565 In order to analyze induction times of increases in histone modifications and Pol2 binding, we  
566 defined the induction time of a feature as the first time point at which a significant increase was  
567 observed compared to its original basal levels (at 0h). Significant increases were defined using an  
568 approach similar to methods such as by DESeq and voom [56,57], which evaluate changes between  
569 samples taking into account the expected variance or dispersion in read counts in function of mean  
570 read counts. This approach is necessary because regions with low read counts typically experience  
571 high fold-changes because of statistical noise in the data. Here we slightly modified this approach to  
572 be applicable to our data (10 time points without replicates; ppm values per promoter/enhancer  
573 region).

574 The values of all histone modifications, Pol2, RNA-seq, TSS-seq reads (ppms, for each time point)  
575 were collected for all promoters (region -1kb to +1kb) and enhancers (entire enhancer region or  
576 region -1kb to +1kb around the enhancer center for enhancers < 2 kb in size). For each feature (all  
577 histone modifications and Pol2 binding), we calculated the median and standard deviation in ppm  
578 values for each region, over the 10 time points. Dispersion was defined as follow:

$$579 \quad d_{x,f} = \left( \frac{s_{x,f}}{m_{x,f}} \right)^2 \quad (1)$$

580 where  $d_{x,f}$ ,  $s_{x,f}$ , and  $m_{x,f}$  represent the dispersion, standard deviation, and median of feature  $f$  in  
581 region  $x$  over the 10 time points of the time series. Fitting a second order polynomial function on the  
582  $\log(d_{x,f})$  as a function of  $\log(m_{x,f})$  for all promoter and enhancer regions, we obtained expected  
583 dispersion values in function of median ppm value (see for example Fig. S20 for H3K9K14ac). From  
584 fitted dispersion values, fitted standard deviation values  $s_{x,f,fitted}$  were calculated (see Eq. 1), and  
585 0h-based Z-scores were calculated as follows:

$$586 \quad Z_{x,f,t} = \frac{(ppm_{x,f,t} - ppm_{x,f,0h})}{s_{x,f,fitted}} \quad (2)$$

587 where  $Z_{x,f,t}$  is the Z-score of feature  $f$  in region  $x$  at time point  $t$ , and  $ppm_{x,f,t}$  is the ppm value  
588 of feature  $f$  in region  $x$  at time point  $t$ . The induction time of a feature  $f$  at region  $x$  was defined as  
589 the first time point where  $Z_{x,f,t} \geq 4$ . To further exclude low-signal regions we added this additional  
590 threshold: the region should have a ppm value  $\geq$  the 25 percentile of non-0 values in at least 1 time  
591 point. If Z-scores did not exceed 4 at any time point, the feature was regarded as not induced at a  
592 region. We used a similar approach to define LPS-induced promoters using TSS-seq data (see below).  
593 For the analysis of induction times of H3K9K14ac, H3K4me3, and H3K36me3 at enhancers in function  
594 of their pre-stimulation basal levels (Fig. S7), we divided promoters into three classes according to  
595 their basal levels of each modifications as follows: Promoters lacking a modifications altogether (0  
596 tag reads after correction described above) were considered as one class (“absent”). The remaining  
597 promoters were sorted according to their basal level of the modification, and were divided into two  
598 classes (“low basal level”, and “high basal level”) containing the same number of promoters.

#### 599 Definition of LPS-induced promoters, unchanged promoters

600 LPS-induced promoters were defined using TSS-seq ppm values. LPS-induced promoters should have  
601  $Z_{x,TSS-seq,t} \geq 4$  for at least 1 time point and have TSS-seq ppm  $\geq 1$  at at least 1 time point. Only TSS-  
602 seq reads aligned in the sense orientation were considered for this (e.g. they should fit the  
603 orientation of the associated gene). For each of the thus obtained 1,413 LPS-induced promoters, the  
604 transcription induction time was defined as the first time point for which  $Z_{x,TSS-seq,t} \geq 4$  was  
605 observed. Unchanged promoters were defined as those promoters having absolute values of  
606  $Z_{x,TSS-seq,t} < 1$  for all time points, leading to 772 promoters.

#### 607 RNA-seq data processing for wild type, *Trif*<sup>-/-</sup> and *Myd88*<sup>-/-</sup> cells

608 RNA-seq data for mouse BM-DCs treated with LPS were obtained from the study by Patil *et al.* [58]  
609 (SRA accession number DRA001131). This data includes time series data for WT, as well as *Trif*<sup>-/-</sup> mice  
610 and *Myd88*<sup>-/-</sup> mice.

611 Mapping of RNA-seq data was performed using TopHat (version 2.0.6) and Bowtie2 (version 2.0.2)  
612 [50,59]. Mapped reads were converted to RPKM values [60] using gene annotation data provided by  
613 TopHat. RNA-seq data obtained from the *Myd88*<sup>-/-</sup> and *Trif*<sup>-/-</sup> mice was processed in the same way.  
614 RPKM values were subjected to quantile normalization over all 10 time points.  
615 For genes corresponding to the LPS-induced promoters, the maximum fold-induction was calculated  
616 in the WT RNA-seq data. The same was done in the *Trif*<sup>-/-</sup> RNA-seq data, and in the *Myd88*<sup>-/-</sup> RNA-seq  
617 data. TRIF-dependent genes were defined as genes for which the fold-induction was more than 5  
618 times lower in the *Trif*<sup>-/-</sup> data than in WT, leading to 141 TRIF-dependent genes (see Fig. 6A). Similarly,  
619 66 MyD88-dependent genes (not shown) were defined as having more than 5 times lower induction  
620 in the *Myd88*<sup>-/-</sup> than in WT.

## 621 Fisher's exact test

622 We used Fisher's exact test to evaluate the significance of differences between induced and non-  
623 induced promoters and enhancers (Fig. 1A,B), the significance of associations between changes of  
624 pairs of features (Fig. 1C,D), and the association between TF binding and increases in histone  
625 modifications, Pol2 binding and transcription (Fig. 4 and Fig. S14).

## 626 List of abbreviations

627	BM-DC	bone marrow-derived dendritic cells
628	DC	dendritic cell
629	FDR	false discovery rate
630	GM-CSF	granulocyte/monocyte colony stimulating factor
631	IFN	interferon
632	IFNR	interferon receptor
633	KO	knock out
634	LPS	lipopolysaccharide
635	Pol2	RNA polymerase II
636	ppm	reads per million reads
637	RPKM	reads per kilobase per million reads
638	TF	transcription factor
639	TLR	Toll-like receptor
640	TSS	transcription start site

641 WCE whole cell extract  
642 WT wild type

## 643 [Declarations](#)

### 644 [Ethics approval and consent to participate](#)

645 Not applicable.

### 646 [Consent for publication](#)

647 Not applicable.

### 648 [Availability of data and materials](#)

649 The ChIP-seq datasets generated and analysed during the current study are available in the DDBJ  
650 repository, accession number DRA004881.

### 651 [Competing interests](#)

652 The authors declare that they have no competing interests.

## 653 [Funding](#)

654 This work was supported by the Japan Society for the Promotion of Science (JSPS) through the  
655 “Funding Program for World-Leading Innovative R&D on Science and Technology (FIRST Program)”,  
656 initiated by the Council for Science and Technology Policy (CSTP), and by a Kakenhi Grant-in-Aid for  
657 Scientific Research (JP23710234) from the Japan Society for the Promotion of Science.

## 658 [Authors' contributions](#)

659 AV, YK, YS, and KN designed the project. YK, ML and YS conducted ChIP-seq experiments, and YK  
660 additional experiments. AV and YK performed data analysis. All authors contributed to the  
661 interpretation of the data. AV and YK wrote the manuscript. All authors read and approved the final  
662 manuscript.

## 663 Acknowledgements

664 We thank the members of the Immunology Frontier Research Center (IFReC) Immuno-Genomics  
665 Research Unit and the Quantitative Immunology Research Unit for helpful discussions and advice, A.  
666 Yoshimura, E. Kurumatani, Y. Kimura, A. Yamashita, K. Imamura, K. Abe and T. Horiuchi for technical  
667 assistance and M. Ogawa for secretarial assistance. Computational time was provided by the  
668 computer cluster of the IFReC Laboratory of Systems Immunology.

## 669 References

- 670 1. Henikoff S. Nucleosome destabilization in the epigenetic regulation of gene expression. *Nat Rev*  
671 *Genet.* 2008;9:15–26.
- 672 2. Greer EL, Shi Y. Histone methylation: a dynamic mark in health, disease and inheritance. *Nat. Rev.*  
673 *Genet.* 2012;13:343–57.
- 674 3. Mercer EM, Lin YC, Benner C, Jhunjunwala S, Dutkowski J, Flores M, et al. Multilineage priming of  
675 enhancer repertoires precedes commitment to the B and myeloid cell lineages in hematopoietic  
676 progenitors. *Immunity.* 2011;35:413–25.
- 677 4. Winter DR, Amit I. The role of chromatin dynamics in immune cell development. *Immunol. Rev.*  
678 2014;261:9–22.
- 679 5. Creighton MP, Cheng AW, Welstead GG, Kooistra T, Carey BW, Steine EJ, et al. Histone H3K27ac  
680 separates active from poised enhancers and predicts developmental state. *Proc. Natl. Acad. Sci. U. S.*  
681 *A.* 2010;107:21931–6.
- 682 6. Kaikkonen MU, Spann NJ, Heinz S, Romanoski CE, Allison K a, Stender JD, et al. Remodeling of the  
683 enhancer landscape during macrophage activation is coupled to enhancer transcription. *Mol. Cell.*  
684 2013;51:310–25.
- 685 7. Ostuni R, Piccolo V, Barozzi I, Polletti S, Termanini A, Bonifacio S, et al. Latent enhancers activated  
686 by stimulation in differentiated cells. *Cell.* 2013;152:157–71.

- 687 8. Voss TC, Hager GL. Dynamic regulation of transcriptional states by chromatin and transcription  
688 factors. *Nat. Rev. Genet.* 2014;15:69–81.
- 689 9. Álvarez-Errico D, Vento-Tormo R, Sieweke M, Ballestar E. Epigenetic control of myeloid cell  
690 differentiation, identity and function. *Nat. Rev. Immunol.* 2014;15:7–17.
- 691 10. Heinz S, Benner C, Spann N, Bertolino E, Lin YC, Laslo P, et al. Simple combinations of lineage-  
692 determining transcription factors prime cis-regulatory elements required for macrophage and B cell  
693 identities. *Mol. Cell.* 2010;38:576–89.
- 694 11. Foster SL, Hargreaves DC, Medzhitov R. Gene-specific control of inflammation by TLR-induced  
695 chromatin modifications. *Nature.* 2007;447:972–8.
- 696 12. Smale ST, Tarakhovsky A, Natoli G. Chromatin contributions to the regulation of innate immunity.  
697 *Annu. Rev. Immunol.* 2014;32:489–511.
- 698 13. Ghisletti S, Barozzi I, Mietton F, Polletti S, De Santa F, Venturini E, et al. Identification and  
699 characterization of enhancers controlling the inflammatory gene expression program in  
700 macrophages. *Immunity.* 2010;32:317–28.
- 701 14. Natoli G. Control of NF- $\kappa$ B-dependent Transcriptional Responses by Chromatin Organization.  
702 *Cold Spring Harb Perspect Biol.* 2009;1:1–11.
- 703 15. Henikoff S, Shilatifard A. Histone modification: Cause or cog? *Trends Genet.* 2011;27:389–96.
- 704 16. Ivashkiv LB, Park SHO. Epigenetic Regulation of Myeloid Cells. *Microbiol Spectr.* 2016;4.
- 705 17. Miller T, Krogan NJ, Dover J, Tempst P, Johnston M, Greenblatt JF, et al. COMPASS: A complex of  
706 proteins associated with a trithorax-related SET domain protein. *Proc. Natl. Acad. Sci. U. S. A.*  
707 2001;98:12902–7.
- 708 18. Pavri R, Zhu B, Li G, Trojer P, Mandal S, Shilatifard A, et al. Histone H2B Monoubiquitination  
709 Functions Cooperatively with FACT to Regulate Elongation by RNA Polymerase II. *Cell.* 2006;125:703–  
710 17.

- 711 19. Stasevich TJ, Hayashi-Takanaka Y, Sato Y, Maehara K, Ohkawa Y, Sakata-Sogawa K, et al.  
712 Regulation of RNA polymerase II activation by histone acetylation in single living cells. *Nature*.  
713 2014;516:272–5.
- 714 20. Kawai T, Akira S. The role of pattern-recognition receptors in innate immunity: update on Toll-  
715 like receptors. *Nat. Immunol.* 2010;11:373–84.
- 716 21. Hoshino K, Kaisho T, Iwabe T, Takeuchi O, Akira S. Differential involvement of IFN- in Toll-like  
717 receptor-stimulated dendritic cell activation. *Int. Immunol.* 2002;14:1225–31.
- 718 22. Liang K, Suzuki Y, Kumagai Y, Nakai K. Analysis of changes in transcription start site distribution  
719 by a classification approach. *Gene*. 2014;537:29–40.
- 720 23. Rabani M, Raychowdhury R, Jovanovic M, Rooney M, Stumpo DJ, Pauli A. Resource High-  
721 Resolution Sequencing and Modeling Identifies Distinct Dynamic RNA Regulatory Strategies. *Cell*.  
722 2014;159:1698–710.
- 723 24. Kumagai Y, Vandenberg A, Teraguchi S, Akira S, Suzuki Y. Genome-wide map of RNA degradation  
724 kinetics patterns in dendritic cells after LPS stimulation facilitates identification of primary sequence  
725 and secondary structure motifs in mRNAs. *BMC Genomics*. 2016;17:127–40.
- 726 25. Garber M, Yosef N, Goren A, Raychowdhury R, Thielke A, Guttman M, et al. A High-Throughput  
727 Chromatin Immunoprecipitation Approach Reveals Principles of Dynamic Gene Regulation in  
728 Mammals. *Mol. Cell*. 2012;47:810–22.
- 729 26. Illingworth RS, Bird AP. CpG islands--'a rough guide'. *FEBS Lett.* 2009;583:1713–20.
- 730 27. Schübeler D, MacAlpine DM, Scalzo D, Wirbelauer C, Kooperberg C, Van Leeuwen F, et al. The  
731 histone modification pattern of active genes revealed through genome-wide chromatin analysis of a  
732 higher eukaryote. *Genes Dev.* 2004;18:1263–71.
- 733 28. Ernst J, Kheradpour P, Mikkelson TS, Shores N, Ward LD, Epstein CB, et al. Mapping and analysis  
734 of chromatin state dynamics in nine human cell types. *Nature*. 2011;473:43–9.

- 735 29. Barski A, Cuddapah S, Cui K, Roh T-Y, Schones DE, Wang Z, et al. High-resolution profiling of  
736 histone methylations in the human genome. *Cell*. 2007;129:823–37.
- 737 30. Arner E, Daub CO, Vitting-Seerup K, Andersson R, Lilje B, Drabløs F, et al. Transcribed enhancers  
738 lead waves of coordinated transcription in transitioning mammalian cells. *Science*. 2015;347:1010–5.
- 739 31. Ramana C V, Chatterjee-Kishore M, Nguyen H, Stark GR. Complex roles of Stat1 in regulating  
740 gene expression. *Oncogene*. 2000;19:2619–27.
- 741 32. Lim CA, Yao F, Wong JJY, George J, Xu H, Chiu KP, et al. Genome-wide Mapping of RELA(p65)  
742 Binding Identifies E2F1 as a Transcriptional Activator Recruited by NF-κB upon TLR4 Activation. *Mol.*  
743 *Cell*. 2007;27:622–35.
- 744 33. Toshchakov V, Jones BW, Perera P-Y, Thomas K, Cody MJ, Zhang S, et al. TLR4, but not TLR2,  
745 mediates IFN-beta-induced STAT1alpha/beta-dependent gene expression in macrophages. *Nat.*  
746 *Immunol*. 2002;3:392–8.
- 747 34. Hirotsu T, Yamamoto M, Kumagai Y, Uematsu S, Kawase I, Takeuchi O, et al. Regulation of  
748 lipopolysaccharide-inducible genes by MyD88 and Toll/IL-1 domain containing adaptor inducing IFN-  
749 beta. *Biochem. Biophys. Res. Commun*. 2005;328:383–92.
- 750 35. Weintraub H, Groudine M. Chromosomal Subunits in Active Genes Have an Altered  
751 Conformation. *Science*. 1976;193:848–56.
- 752 36. Lenhard B, Sandelin A, Carninci P. Metazoan promoters: emerging characteristics and insights  
753 into transcriptional regulation. *Nat. Rev. Genet*. 2012;13:233–45.
- 754 37. Kayama H, Ramirez-Carrozzi VR, Yamamoto M, Mizutani T, Kuwata H, Iba H, et al. Class-specific  
755 regulation of pro-inflammatory genes by MyD88 pathways and IκBζ. *J. Biol. Chem*. 2008;283:12468–  
756 77.
- 757 38. Tartey S, Matsushita K, Vandenbon A, Ori D, Imamura T, Mino T, et al. Akirin 2 is critical for  
758 inducing inflammatory genes by bridging IκB-ζ and the SWI / SNF complex. *EMBO J*. 2014;33:2332–



- 759 48.
- 760 39. Chen X, Barozzi I, Termanini A, Prosperini E, Recchiuti A, Dalli J, et al. Requirement for the histone  
761 deacetylase Hdac3 for the inflammatory gene expression program in macrophages. *Proc. Natl. Acad.*  
762 *Sci. U. S. A.* 2012;109:2865–74.
- 763 40. Zhu Y, van Essen D, Sacconi S. Cell-Type-Specific Control of Enhancer Activity by H3K9  
764 Trimethylation. *Mol. Cell.* 2012;46:408–23.
- 765 41. Austenaa L, Barozzi I, Chronowska A, Termanini A, Ostuni R, Prosperini E, et al. The Histone  
766 Methyltransferase Wbp7 Controls Macrophage Function through GPI Glycolipid Anchor Synthesis.  
767 *Immunity.* 2012;36:572–85.
- 768 42. Vahedi G, Takahashi H, Nakayamada S, Sun H, Sartorelli V, Kanno Y, et al. STATs Shape the Active  
769 Enhancer Landscape of T Cell Populations. *Cell.* 2012;151:981–93.
- 770 43. Qiao Y, Giannopoulou EG, Chan CH, Park S-H, Gong S, Chen J, et al. Synergistic activation of  
771 inflammatory cytokine genes by interferon- $\gamma$ -induced chromatin remodeling and toll-like receptor  
772 signaling. *Immunity.* 2013;39:454–69.
- 773 44. MacQuarrie KL, Fong AP, Morse RH, Tapscott SJ. Genome-wide transcription factor binding:  
774 beyond direct target regulation. *Trends Genet.* 2011;27:141–8.
- 775 45. Weiner A, Hsieh T-HS, Appleboim A, Chen H V, Rahat A, Amit I, et al. High-Resolution Chromatin  
776 Dynamics during a Yeast Stress Response. *Mol. Cell.* 2015;58:371–86.
- 777 46. Drouin S, Laramé e L, Jacques P-E', Forest A, Bergeron M, Robert F. DSIF and RNA polymerase II  
778 CTD phosphorylation coordinate the recruitment of Rpd3S to actively transcribed genes. *PLoS Genet.*  
779 2010;6:1–12.
- 780 47. Yamamoto M, Sato S, Hemmi H. Role of Adaptor TRIF in the MyD88-Independent Toll-Like  
781 Receptor Signaling Pathway. *Science.* 2003;301:640–3.
- 782 48. Saitoh T, Satoh T, Yamamoto N, Uematsu S, Takeuchi O, Kawai T, et al. Antiviral protein viperin

- 783 promotes toll-like receptor 7- and toll-like receptor 9-mediated type i interferon production in  
784 plasmacytoid dendritic cells. *Immunity*. 2011;34:352–63.
- 785 49. Hemmi H, Kaisho T, Takeda K, Akira S. The Roles of Toll-Like Receptor 9, MyD88, and DNA-  
786 Dependent Protein Kinase Catalytic Subunit in the Effects of Two Distinct CpG DNAs on Dendritic Cell  
787 Subsets. *J. Immunol*. 2003;170:3059–64.
- 788 50. Langmead B, Salzberg SL. Fast gapped-read alignment with Bowtie 2. *Nat. Methods*. 2012;9:357–  
789 9.
- 790 51. Li H, Handsaker B, Wysoker A, Fennell T, Ruan J, Homer N, et al. The Sequence Alignment/Map  
791 format and SAMtools. *Bioinformatics*. 2009;25:2078–9.
- 792 52. Feng J, Liu T, Qin B, Zhang Y, Liu XS. Identifying ChIP-seq enrichment using MACS. *Nat. Protoc*.  
793 2012;7:1728–40.
- 794 53. Lee B, Bhinge AA, Battenhouse A, Song L, Zhang Z, Grasfeder LL, et al. Cell-type specific and  
795 combinatorial usage of diverse transcription factors revealed by genome-wide binding studies in  
796 multiple human cells. *Genome Res*. 2012;22:9–24.
- 797 54. Tsuchihara K, Suzuki Y, Wakaguri H, Irie T, Tanimoto K, Hashimoto S, et al. Massive  
798 transcriptional start site analysis of human genes in hypoxia cells. *Nucleic Acids Res*. 2009;37:2249–  
799 63.
- 800 55. Meyer LR, Zweig AS, Hinrichs AS, Karolchik D, Kuhn RM, Wong M, et al. The UCSC Genome  
801 Browser database: extensions and updates 2013. *Nucleic Acids Res*. 2013;41:D64–9.
- 802 56. Anders S, Huber W. Differential expression analysis for sequence count data. *Genome Biol*.  
803 2010;11:R106.
- 804 57. Law CW, Chen Y, Shi W, Smyth GK. voom : precision weights unlock linear model analysis tools  
805 for RNA-seq read counts. 2014;1–17.
- 806 58. Patil A, Kumagai Y, Liang K-C, Suzuki Y, Nakai K. Linking transcriptional changes over time in

807 stimulated dendritic cells to identify gene networks activated during the innate immune response.  
808 PLoS Comput. Biol. 2013;9:e1003323.  
809 59. Kim D, Pertea G, Trapnell C, Pimentel H, Kelley R, Salzberg SL. TopHat2: accurate alignment of  
810 transcriptomes in the presence of insertions, deletions and gene fusions. Genome Biol. 2013;14:R36.  
811 60. Mortazavi A, Williams B a, McCue K, Schaeffer L, Wold B. Mapping and quantifying mammalian  
812 transcriptomes by RNA-Seq. Nat. Methods. 2008;5:621–8.

## 813 Figure Legends

814 **Figure 1:** Frequencies of induction of features at LPS-induced promoters. (A) Heatmap showing the  
815 changes (white: no change; red: induction; blue: repression) in transcriptional activity of 1,413 LPS-  
816 induced promoters, relative to time point 0h. At the right, induction times and the number of  
817 promoters induced at each time point are indicated. (B) The fraction of promoters (y-axis) with  
818 increases in features (x-axis) are shown for the genome-wide set of promoters (green), and for the  
819 LPS-induced promoters (orange). Increases in H3K4me3, H3K9K14ac, H3K27ac, H3K36me3, RNA, and  
820 Pol2 binding are observed relatively frequently at LPS-induced promoters. Significance of differences  
821 was estimated using Fisher's exact test; \*:  $p < 1e-4$ ; \*\*:  $p < 1e-6$ ; \*\*\*:  $p < 1e-10$ . (C) Same as (B), for  
822 enhancers. (D-E) Heatmaps indicating the overlap in induction of pairs of features. Colors represent  
823 p values ( $-\log_{10}$ ) of Fisher's exact test. White: low overlap; Red: high overlap. Plots are shown for  
824 promoters (D), and enhancers (E).

825

826 **Figure 2:** Induction times of transcription, Pol2 binding and histone modifications at promoters in  
827 function of induction of transcriptional activation times. (A-F) The fraction (top) and cumulative  
828 fraction (bottom) of promoters with an induction in RNA-seq reads (A), Pol2 binding (B), H3K9K14ac  
829 (C), H3K4me3 (D), H3K36me3 (E), and H3K27ac (F) are shown. Line colors represent promoters with  
830 different transcriptional activation times. Black boxes indicate time frames with frequent induction  
831 of a feature.

832

833 **Figure 3:** Induction times of RNA-seq reads (A), Pol2 binding (B), H3K9K14ac (C), and H3K27ac (D) at  
834 enhancers of LPS-induced promoters. Axes and color codes are the same as in Fig. 2.

835

836 **Figure 4:** Associations between LPS-induced TF binding at promoters (left) and enhancers (right) and  
837 increases in histone modifications, Pol2 binding and transcription at the newly bound regions. Colors  
838 in the heatmap represent the degree of co-occurrence (Fisher's exact test,  $-\log_{10}$  p values) between  
839 new TF binding events (rows) and increases (columns). TFs (rows) have been grouped through  
840 hierarchical clustering by similarity of their association pattern.

841

842 **Figure 5:** Interaction between STAT1 binding and accumulation of H3K9K14ac and H3K4me3. (A) For  
843 all genomic regions bound by STAT1 at 2h after LPS stimulation, mean H3K9K14ac signals are shown  
844 over time. Left: profile of mean values (y axis) over time in bins of 100 bps in function of distance (x  
845 axis) to the TF binding site. Right: mean values (y axis) summed over the region -2kb to +2kb over all  
846 bound regions, over time (x axis). The red arrow indicates the time at which these regions become  
847 bound by STAT1. (B) The fraction of promoters with induction of H3K9K14ac over time after  
848 stimulation (x axis). Blue: regions bound by STAT1 at time 2h. Red: regions not bound by STAT1 at  
849 any time point. Numbers in parentheses show the number of regions bound and not bound by  
850 STAT1 (C) As in (B) for enhancer regions bound (and not bound) by STAT1. (D) As in (A), for H3K4me3  
851 at the genomic regions bound by STAT1 2 hours after LPS stimulation. (E) As in (B), for promoter  
852 regions with induction in H3K4me3.

853

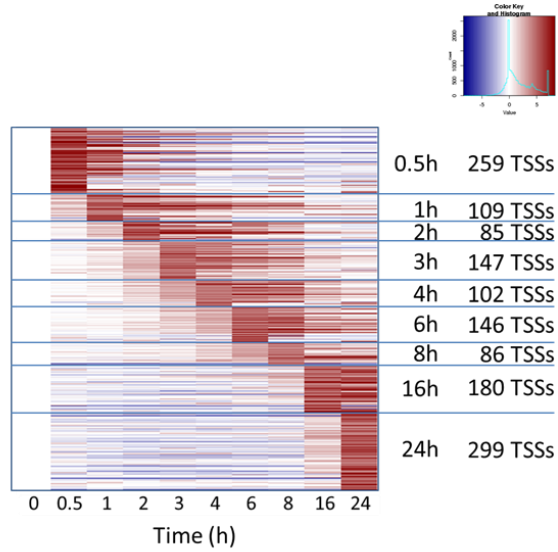
854 **Figure 6:** Increase of H3K9K14ac and H3K4me3 at STAT1/2-bound promoters of TRIF-dependent  
855 genes. (A) Heatmap showing gene expression changes in WT, *Myd88*<sup>-/-</sup>, and *Trif*<sup>-/-</sup> mice after LPS

856 stimulation of mouse DCs for TRIF-dependent genes. (B) TF binding ratios of promoter regions with  
857 stable expression (“unchanged”, blue), all LPS-induced promoters in WT (red), TRIF-dependent  
858 promoters (green), and MyD88-dependent promoters (purple). TRIF-dependent promoters are often  
859 bound by STAT1 and/or STAT2. (C) Fraction of regions with induction of H3K9K14 for TRIF- and  
860 MyD88-dependent promoters. For TRIF-dependent genes, plots are also shown specifically for STAT1  
861 and/or STAT2 bound and unbound regions. Colors of bars indicate the timing of H3K9K14ac  
862 induction. (D) Same as (C) for H3K4me3 induction. Induction of H3K9K14ac and H3K4me3 is highly  
863 specific for STAT1/2 bound TRIF-dependent genes, and concentrated at time points 2-3 h and 2-4 h,  
864 respectively. Percentages indicate the fraction of regions with induction between 2-3 hours for  
865 H3K9K14ac, and between 2-4 hours for H3K4me3.

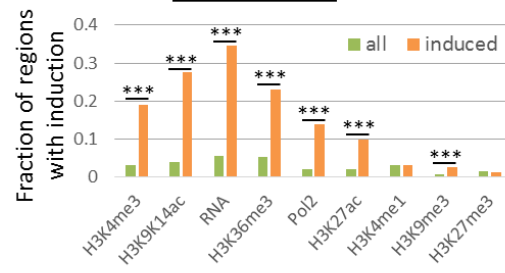
866

867 **Figure 7:** Gene expression (mRNA), H3K9K14ac and H3K4me3 dynamics in WT, *Trif*<sup>-/-</sup>, *Irf3*<sup>-/-</sup>, and *Ifnar*<sup>-/-</sup>  
868 <sup>-/-</sup> cells following LPS stimulation. We distinguished genes of which expression and histone  
869 modifications are independent (A), dependent (B), and partially dependent (C) on TRIF, IRF3, and  
870 IFNR. Error bars represent the standard deviation based on duplicate experiments. The red dotted  
871 line in each graph represents the mean value at 0h. Y axes represent fold induction (for mRNA)  
872 and % input (for H3K9K14ac and H3K4me3). Binding of promoters by RelA, IRF1, STAT1 and STAT2 is  
873 indicated at the right hand side (white: no binding, purple: binding by RelA, green: binding by IRF1,  
874 blue: binding by STAT1, red: binding by STAT2).

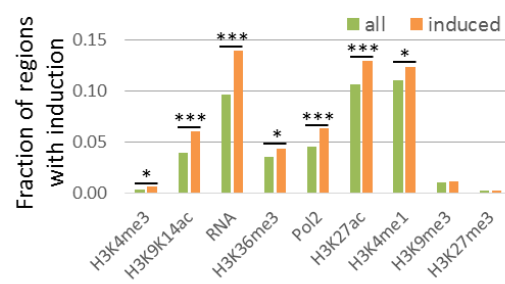
## A LPS-induced promoters



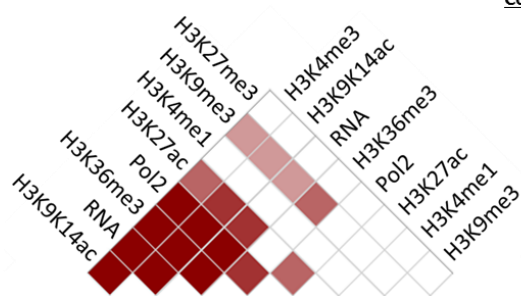
## B Promoters



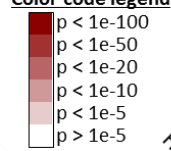
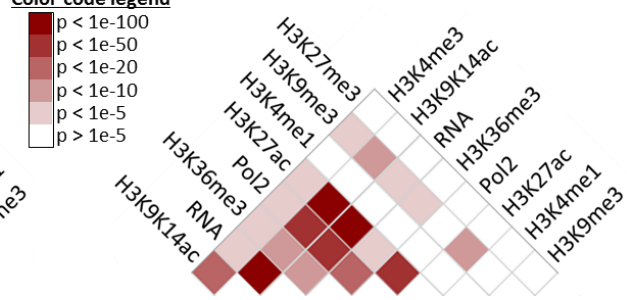
## C Enhancers

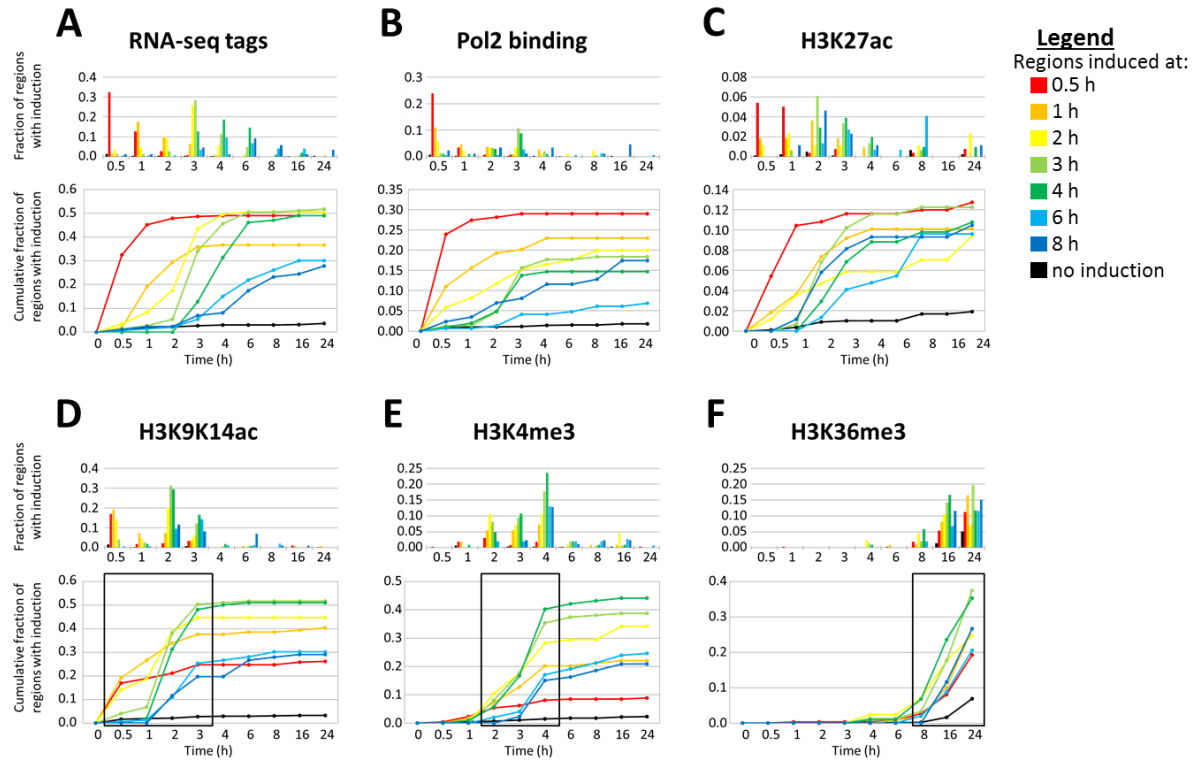


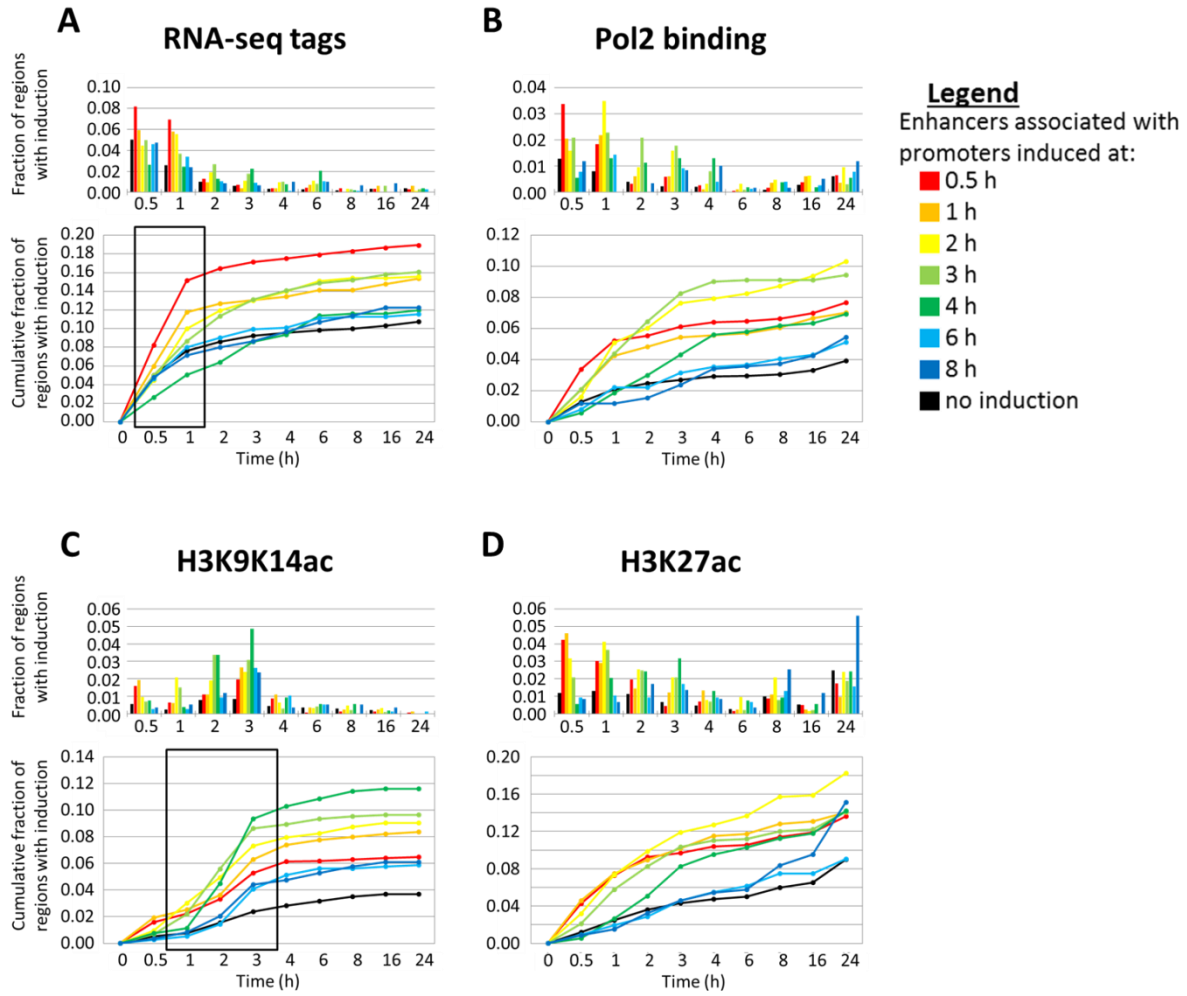
## D Promoters



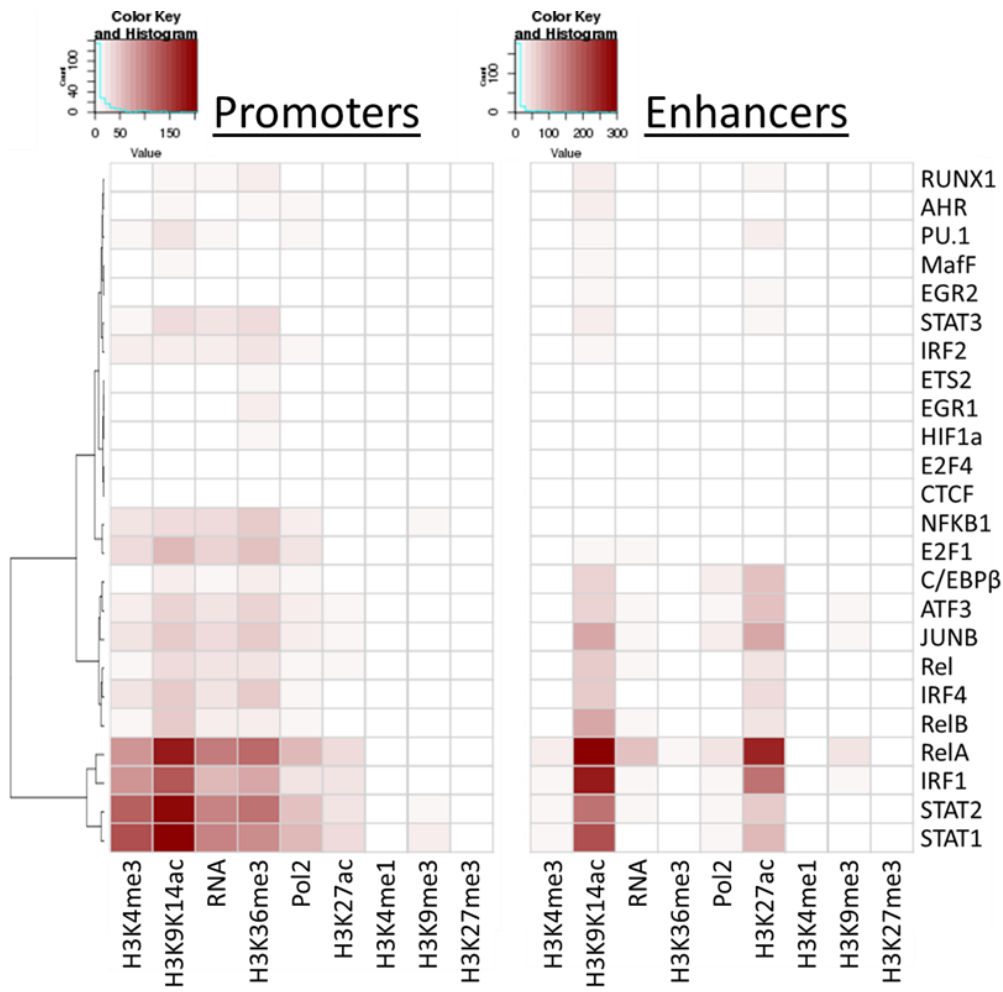
## E Enhancers



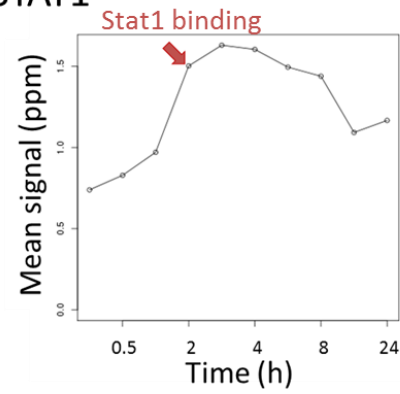
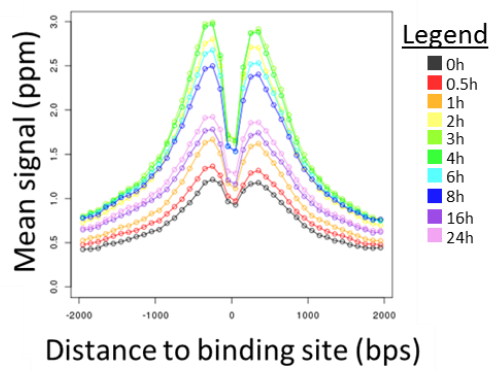




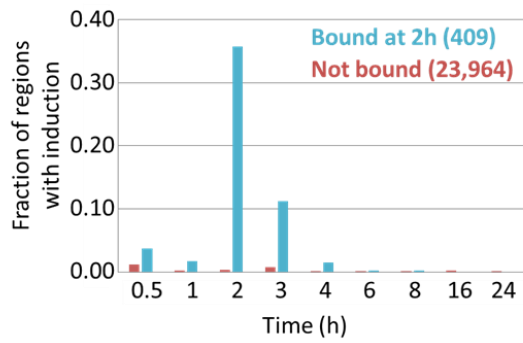




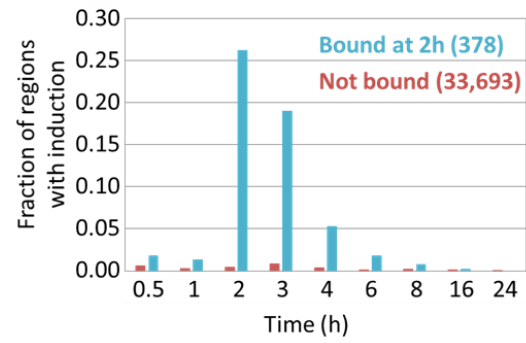
## A H3K9K14ac at loci bound by STAT1



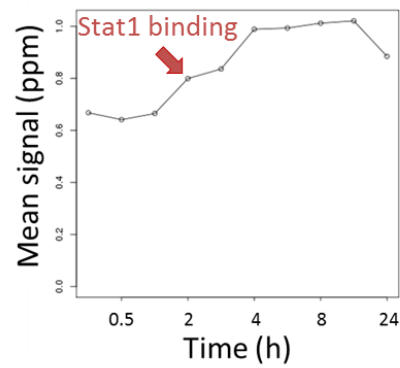
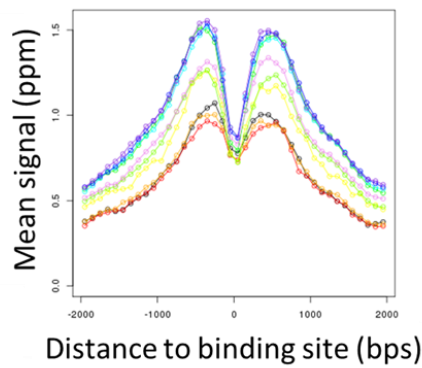
## B Promoters



## C Enhancers



## D H3K4me3 at loci bound by STAT1



## E Promoters

